Energy Transfer at a Gas−Liquid Interface: Kinematics in a Prototypical System

Tamas J. Szabo, Ali Siavosh-Haghighi, and John E. Adams*

Department of Chemistry, University of Missouri-Columbia, Columbia, Missouri 65211-7600

Received: July 16, 2005; In Final Form: November 24, 2005

A detailed characterization of collisional energy transfer at a liquid surface not only provides a framework for the interpretation of experimental studies but also affords insight into energy feedback mechanisms that may be important in multiphase combustion processes. We address this problem by performing simulations of a prototypical Lennard−Jones system, investigating the dependence of the energy transfer and incident-atom trapping probability on the liquid temperature, on the mass and angle of incidence of the impinging atom, and on the strength of the gas−liquid interaction. In general, in agreement with the results of experiments, these calculations point to the dominance of kinematic effects in determining the gross energy transfer, but they also attest to the important role played by surface roughening in the enhancement of energy transfer that accompanies an increase in the liquid temperature.

I. Introduction

One of the characteristics of some burning solid propellants is the appearance of a thin liquid layer at the surface of the propellant. This observation has stimulated the development of multiphase combustion models in which the gasification step is evaporation from this liquid layer, with the multitude of coupled combustion reactions then occurring exclusively in the gas phase.[1−3] Construction of a mathematically closed (1D) continuum model of these processes proceeds by the application of appropriate continuity equations for matter and energy at the phase boundaries, resulting in a formalism that has been remarkably successful in reproducing the burning rate of several practical propellants. Even with the demonstrated success of these continuum models, though, one ultimately would like to move toward a first-principles *molecular* model of the combustion process that would aid in the evaluation of prospective propellant materials. One component of that process is energy feedback from the combustion zone to the interface at which gasification is occurring, and it is this aspect of the problem that has stimulated the present work, which is aimed at characterizing the fundamental aspects of interfacial energy transfer.

Although remarkable progress has been made during the last fifty years in understanding the structure and reactivity of solid surfaces,[4,5] progress prompted largely by the advent of ultrahigh vacuum technology and the subsequent development of a host of surface-sensitive analytical techniques,[6] liquid surfaces have received comparatively little attention. The first such studies, conducted by Hurlbut and Beck,[7] focused exclusively on elastic and inelastic scattering of nonreactive gases from low-melting liquid metals, work that subsequently was extended by Sinha and Fenn[8] to the investigation of a molecular liquid (glycerol) and by Balooch and co-workers a decade later to reactive scattering events (Cl_2 reactions with In,[9] Pb,[10] Bi,[11] and Sn;[12] various gases with U[13,14]). Of the more recent work, that reported by Nathanson and co-workers[15−28] has been particularly instrumental not only in clarifying features of the energy transfer occurring at a gas−liquid interface but also in determining adsorbate residence times and solubilities. We will return to a discussion of particular results emanating from this group, but we call the reader's attention here to a recent review article that summarizes their body of work.[29]

The drive to understand these experimental findings has sparked several theoretical studies of collisions at a gas−liquid interface.[19,20,24,30−32] Given that the liquid−vacuum interface on which the gas molecules impinge is aperiodic, most of these studies have utilized molecular dynamics simulations involving hundreds of condensed-phase atoms, either located in the "bottom" of a larger simulation cell or else found within a lamella occupying the central region of the cell. In the latter case, two interfaces are created, either or both of which may be used as collision targets. (Indeed, this is the approach adopted for the present work, the details of which appear in Section II below.) In contrast, Muis and Manson[31,32] calculated the angular distributions of species reflected at a liquid metal−vacuum interface using classical scattering theory. They noted that for high incident energies, their results obtained in the limit that the dynamics is dominated by single collisions with a vibrating continuum surface were in better agreement with the experimental results than were those deriving from a model that assumes uncorrelated scattering from discrete centers.

The extant theoretical studies, quite reasonably, have focused primarily on reproducing the results of particular experimental measurements involving surfaces of molten metals,[24,30−32] water,[33] glycerol,[20] or squalane.[19] However, we believe that it is worthwhile to take a somewhat longer view of gas−liquid energy transfer, to concentrate not on improving the correspondence of certain computed and measured results but rather on investigating in some detail a simple prototypical system that may yet reveal most or all of the fundamental behavior underlying the dynamics in complex systems. If, for example, the energy transfer in this simple system is found to be dominated by kinematics rather than subtle potential effects and if the simple system appears to mirror the gross dynamics in a variety of real systems, then we can have some confidence that those same kinematic effects will be dominant in the real systems as well. We also would like to be able to take advantage of the insight afforded by characterizations of energy transfer

* Corresponding author. E-mail: AdamsJE@missouri.edu.

10.1021/jp053923v CCC: $33.50
Published on Web 12/31/2005

at gas−solid interfaces inasmuch as so much work already has gone into devising models of those processes. Of course, it will be just as important to determine when caution is warranted in extending such characterizations to the gas−liquid case. Those situations will suggest the most fruitful directions for future investigations.

II. Simulations

We selected a Lennard−Jones atomic system as our model in this study in the expectation that such a system (1) incorporates the most important kinematic effects involved in gas−liquid collision dynamics; (2) yields results that are generalizable to a variety of actual systems by means of the principle of corresponding states; and (3) avoids other possible complications, such as the role that internal degrees of freedom play in energy disposition, which will be relevant in some cases. In examining this particular system ($V_{ij} = 4\epsilon_{ij}[(\sigma_{ij}/r_{ij})^{12} - (\sigma_{ij}/r_{ij})^{6}]$ for the interaction of particles i and j), we can also draw upon the results from previous simulations performed to elucidate certain aspects of the gas−liquid scattering event.[24,30] The parameters adopted here initially were the set suggested by Tribe et al.[24] to describe Ar incident on an In surface: for the liquid species (In), $\epsilon_l/k = 606.8$ K and $\sigma_l = 281$ pm; for the incident species (Ar), $\epsilon_g/k = 119.8$ K and $\sigma_g = 341$ pm; and for the potential "cross terms", the conventional Lorentz−Berthelot combining rules[34] were used, yielding $\epsilon_{gl}/k = 269.6$ K and $\sigma_{gl} = 311$ pm.

Having chosen a force field, we generated initial conditions for the collision dynamics studies following the general prescription suggested by Tribe et al.[24] First, we equilibrated a sample of the neat liquid by means of an *NVT* simulation of 864 atoms at a Lennard−Jones reduced temperature[34] ($T^* = kT/\epsilon$) of 0.85 and reduced density ($\rho^* = \rho\sigma^3$) of 0.85, corresponding in this case to a cubic simulation cell of edge length 2838 pm. In this preliminary equilibration sequence, we began from the fcc crystal lattice, with periodic boundary conditions applied in all dimensions, and used a 6.7 fs time step. Throughout this work, the energy and length scales (respectively, ϵ and σ) used in determining the values of Lennard−Jones reduced quantities were ϵ_l and σ_l. Once the equilibrated liquid had been obtained, the simulation box edge length in the z dimension then was extended by nearly a factor of 3 to 8000 pm, leaving a liquid lamella in the center of the box (now a parallelepiped) and producing two liquid−vacuum interfaces. An *NVE* equilibration of this extended system, again performed using periodic boundary conditions in three dimensions, yielded a final T^* of 0.72. (As a point of reference, this reduced temperature corresponds to 436 K in the case of liquid In.) From this point, we carried out an *NVT* simulation for 2.5×10^5 steps and determined an average density profile along the long axis of the simulation cell. Finally, we generated a library of liquid configurations for use in the subsequent scattering simulations by storing the positions and momenta of the atoms at intervals during a continuation of the previous *NVT* simulation. One hundred distinct configurations were obtained in this manner. All calculations were carried out using the DL_POLY_2 code,[35] with modules being added as necessary to adapt the code to our specific application.

With the initial conditions of the liquid prepared, we turned to the actual energy transfer simulations. The initial position of the incident species was selected at random within a plane parallel to the average position of the liquid surface and at a distance from that surface that lay beyond the range of the Lennard−Jones potential energy cutoffs. (Although each liquid configuration has two surfaces, to date we have only directed species at the $+z$ face of the lamella.) The atom was then directed toward one of the liquid surface configurations with 92 kJ/mol of kinetic energy, roughly equal to 25 *RT* for the system and surface temperature considered here; in terms of a Lennard−Jones reduced energy, $E_i^* = E_i/\epsilon_l = 18.2$, at a selected angle with respect to the surface normal. (Initially, all of the incident atom motion was taken to lie in the xz plane.) An *NVE* trajectory of the system was then calculated, ending when either the initially incident species returned to the plane above the surface or a total time of 14.4 ps had elapsed (1.2×10^4 steps of 1.2 fs). At the end of the trajectory, the kinetic energy of the initially incident atom was determined. If the trajectory time expired prior to the return of the incident atom to the plane above the surface, the atom was labeled "trapped" *unless* its net momentum was carrying it away from the surface *and* the forces on the atom were zero. The latter provision compensates in part for an overestimation of the trapping probability that would arise if the time criterion alone were used: an atom that is scattered to an angle such that its final momentum in the $+z$ direction is small simply takes longer to reach the counting surface. The results reported herein are based on 4000 trajectories for each set of initial conditions.

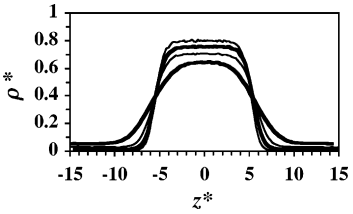

Figure 1. Liquid density profiles determined for liquid temperatures (T^*) of 0.72, 0.76, 0.84, and 0.92, corresponding (in order) to decreasing maximum ρ^* values.

III. Results and Discussion

In beginning the description of our simulation results, we again emphasize that the present work is not designed to provide yet a better fit to a particular set of experimental results than those obtained heretofore. Tribe et al.,[24] for example, have modeled the Ar/In(l) system using the same Lennard−Jones potential functions adopted herein; our own calculations necessarily yield an agreement with experiment that is equivalent to theirs. We thus undertake this work knowing that reproduction of the experimental data in that particular system will not be perfect. (Lennard−Jones potentials applied to the particular case of liquid metals are known to yield surfaces that are rougher than experiments suggest.[30]) Our interest here, however, lies in elaborating the broader range of energy-transfer phenomena expressed when a gas collides with a liquid surface rather than in liquid metals per se.

A. Liquid Surface Contours. The gross structure of our system is revealed by a plot of the average liquid-atom number density versus distance along the z axis, which is the long axis of our simulation cell. Seen in Figure 1 are density plots of this sort for a range of equilibrium liquid temperatures, from $T^* = 0.72$ to 0.92 (436 to 560 K, respectively, in the case of liquid In, for example).

In the case of the lowest temperature investigated here, the surface density profile shown agrees well with the result reported previously by Tribe et al.[24] as expected. Note in particular that the width of the surface region is finite and that it increases with increasing liquid temperature, more than doubling between the lowest and highest temperatures considered. Accompanying

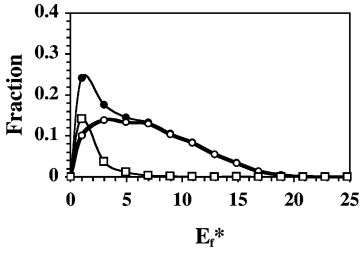

Figure 2. Distribution of final energies for atoms incident on a liquid surface at $T^* = 0.72$ with an initial (Lennard−Jones reduced) energy of 18.2 and an incidence angle of 55°. Results obtained using the full set of 4000 trajectories are shown with closed circles; results obtained using only those trajectories that do not produce trapping are shown with open circles. The difference between these data sets, shown with open squares, is the energy distribution of the trapped species.

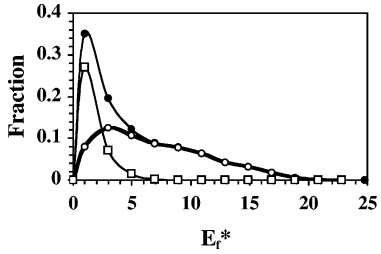

Figure 3. Energy distributions as in Figure 2 but for $T^* = 0.92$.

this expansion of the surface region, which reflects a net roughening of the surface, is the concomitant decrease in the average density of the liquid phase. Consistent with this observation is a shift, albeit a small one, in the position of the Gibbs surface, which can be obtained in the present case using the conventional "equal area" construction.[36] These positions (given here only for the surface lying at positive z) are $z^* = z/\sigma_l = 5.2$, 5.3, 5.5, and 5.7 for the four liquid temperatures, in increasing order, for which results are displayed in Figure 1. One also finds a cautionary note in these results, namely, that a larger system size will be needed in order to push these calculations to a higher temperature, inasmuch as a narrowing of the liquid regime to a thickness of less than $5\sigma_l$ results in the two surfaces of the lamella "seeing" one another.

B. Final Energy Distributions. One does not expect that the collision of gas atoms with a liquid surface will yield only the limiting cases, namely, full thermal equilibration with the surface or elastic scattering. Indeed, a range of behavior is what we find, including a small probability that the surface will impart energy to the incident atom. An example of this behavior is shown in Figure 2, where we give distributions of the final energies of initially incident atoms for an entire set of 4000 collision events and for the subsets of those collision events corresponding to scattering or trapping. (In these calculations, the particle masses chosen correspond to Ar incident on an In surface; the ratio of the masses in this case is therefore $\mu = m/M = 0.348$.)

Certainly, it is no surprise that the scattered and full distributions are essentially identical beyond $E_f^* = 5$. To become trapped at the surface, the incident atom either must lose sufficient energy to fall into the gas−liquid attractive well or else it must be scattered in a direction parallel (or nearly so) to the surface, although this latter situation also increases the likelihood that subsequent collisions will thermalize the atom. At a sufficiently high final kinetic energy, though, the more likely scenario is that the atom simply escapes from the surface, thereby contributing to both of the distributions.

Perhaps the most striking feature of these distributions is that they testify to considerable net energy transfer even in the absence of trapping. This result can be quantified by fitting the kinetic energy distribution of the scattered species to a Maxwell−Boltzmann distribution and extracting a characteristic temperature of these species. For the particular set of initial conditions considered here, this procedure yields a reduced temperature of 3.9, which may then be compared to the initial reduced energy of 18.2. Using these data to compute a thermal accommodation coefficient[37] for the scattered atoms is not strictly valid, the initial energy distribution is a delta function rather than being characterized by a thermal distribution, but one does get a rough measure of the effect by writing $\alpha = (T_i^* - T_f^*)/(T_i^* - T_l^*)$ and finding that in the present case $\alpha = 0.8$. One might find it surprising that with such a large value of α the majority of incident atoms nonetheless are scattered from the surface, but it is important to remember that the well depth of the two-body gas−liquid potential is only 0.4443 (in reduced energy units). Energy transfer must be very efficient indeed for an atom to become trapped; fitting the kinetic energy distribution of the trapped species to a Maxwell−Boltzmann distribution yields a characteristic temperature of 0.84, which exceeds the bulk liquid temperature by only 0.12.

This efficiency of energy transfer suggested by the results shown in Figure 2 could arise in various ways, but in the case of a liquid surface, one is prone to attribute this efficiency in part to multiple collisions with a thermally roughened surface.[38] If that is the case, then one should expect that increased roughening will be accompanied by greater net energy transfer. In Figure 3, we show energy distributions such as those given in Figure 2, but in this case corresponding to a reduced liquid temperature of 0.92.

Immediately one sees that at the higher liquid temperature, the fraction of atoms having final energies that fall within the lowest energy bin is about 40% greater than what was found at the lower temperature (0.72). Again fitting the final energy distributions of trapped and scattered atoms to a Maxwell−Boltzmann distribution, we find that a characteristic reduced temperature of 0.82 describes the energy distribution of the trapped species (this is slightly less than the value that was found in the case of the lower surface temperature) and a temperature of 3.7 describes the scattered-atom results. (The thermal accommodation coefficient for the scattered atoms again is about 0.8.) Here the fitted temperature of the trapped species is calculated to be even lower than the bulk liquid temperature, but some caution is warranted in interpreting this result. The distribution of trapped-species kinetic energies is strongly peaked at low energies, and therefore the rather course-grained binning of these final energies could have a significant effect on the calculation of a characteristic temperature. Nonetheless, the important points are that the net energy transfer increases with increasing liquid temperature and that this behavior is associated with an increased probability of trapping at the higher-temperature surface.

C. Incident Angle Dependence. In modeling the energy feedback from a gas-phase combustion process to the surface of a liquid fuel source, one must account for the fact that the incident species will impact the surface with the entire range of incidence angles. To probe the dependence of the net energy transfer on the angle of incidence, we have investigated three different specific incident angles: 55° (the angle used in the calculations described previously), 30°, and 0°. The energy distributions for the scattered and trapped species resulting from these simulations are displayed in Figure 4.

The effect on the general shape of the energy distributions arising from changing the initial angle of incidence is seen to

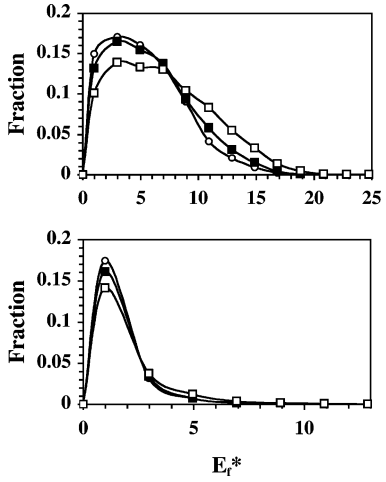

Figure 4. Final energy distributions for scattered (upper panel) and trapped (lower panel) species initially incident at angles of 0° (open circles), 30° (solid squares), and 55° (open squares). The liquid temperature here is $T^* = 0.72$.

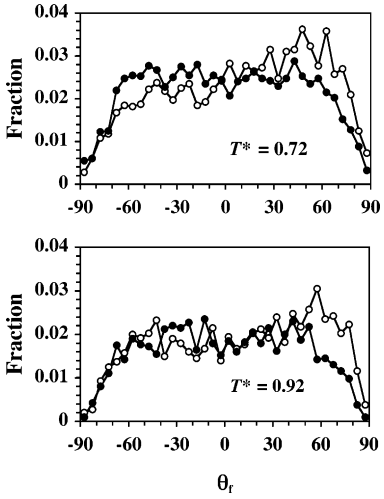

Figure 5. Final scattering angle distributions for incident angles of 0° (closed circles) and 55° (open circles) at two liquid temperatures.

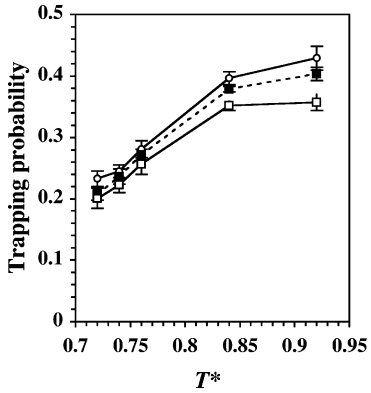

Figure 6. Incident-atom trapping probabilities for incidence angles of 0° (open circles), 30° (solid squares), and 55° (open squares). Error bars correspond to one standard deviation.

be small here; nonetheless, one does find a somewhat greater net energy transfer when the impinging particle approaches the surface at an angle closer to normal incidence. This result implies a propensity for transfer of momentum perpendicular to the liquid surface, but one should not conclude that a simple "cube" model[39,40] based on conservation of parallel momentum, which can be useful in characterizing gas−solid energy transfer, will be adequate in understanding the gas−liquid collision process. However, extended models of this sort such as Tully's "washboard" model[41] may find more applicability, inasmuch as they include surface corrugation, although one then needs to be wary about the inclusion of spurious periodicity effects.

As one would expect, the energy distribution of the trapped species is essentially invariant with respect to the angle of incidence, for in each case the majority of the incident atom's energy must be transferred to the surface atoms if trapping is to occur. That the magnitude of the peak appearing in the lower panel of Figure 4 decreases with increasing angle of incidence confirms the inverse dependence of the energy transfer, and hence of the trapping probability, on θ_i. However, the relatively small differences seen here suggest that trapping is a consequence of multiple collisions, inasmuch as only the initial two-body collision event is expected to retain the signature of the initial approach angle.

Corroboration of this result, that many gas−liquid collision events involve multiple collisions, may be found in the angular distributions of the atoms scattered from the liquid surface, which are given in Figure 5. For all of the initial conditions investigated, the scattering angle distributions are broad, indicative of very significant energy transfer and multiple collision events. The distributions deriving from collisions at normal incidence are approximately symmetric, forward and backward, whereas those corresponding to an incidence angle of 55° exhibit modest peaking in the forward direction. It is important to note here that the lack of smoothness in the angular distributions reflects real statistical fluctuations of 20−30%, so it would be a mistake to make too much of a structure seen in these plots. Nevertheless, the general patterns are entirely consistent with the degree of energy transfer revealed in Figures 2−4. The liquid temperature dependence here is not dramatic, save for the generally smaller peak heights generated at the higher temperature (recall that Figure 3 indicates that there is a higher probability of trapping at this temperature, and thus fewer atoms are scattered); the only notable trend is the slightly stronger tendency for forward scattering near the specular angle.

D. Trapping Probabilities. Several of the measures of energy transfer discussed thus far have attested to the dependence on the liquid temperature and the angle of incidence of the probability that the incident atom will become trapped and thermally equilibrated at the liquid surface. As we mentioned in Section II above, an initially incident atom in our simulations is tagged as "trapped" if within a fixed period of time that atom has not been scattered from the surface nor is it moving away from the surface free of interactions with surface atoms. The energy profiles of the trapped atoms shown in Figures 2 and 3 afford some assurance that those atoms indeed are thermally equilibrated (or nearly so) with the liquid atoms and that our trapping criterion is reasonable. The summary of these trapping probability calculations is shown in Figure 6.

For each of the three angles of incidence studied, the trapping probability is found to double (roughly) over a reduced temperature range of 0.20. (To put this temperature range into perspective, we note that for the parameters appropriate to liquid In, it translates into a difference of 124 K between the highest and lowest temperatures.) This nonlinear temperature dependence appears to become a little stronger as the angle of incidence is decreased, there being little difference in the trapping at the two highest temperatures studied in the case of 55° incidence, while the results are still trending upward over that range for smaller angles of incidence. An interesting feature of the results obtained at $T^* = 0.84$ and 0.92 is that they vary

linearly with the normal component of the initial projectile energy, that is, with $E = E_i \cos \theta_i$. It is tempting, therefore, to draw a parallel between these results and the simple models of gas−solid energy transfer that focus exclusively on that same component of the initial energy.[39,40] However, given the limited amount of data at this point and the fact that this scaling does not obtain over the entire temperature range considered, we shall only note the observation and suggest that the result is worthy of further study.

E. Mass and Potential Energy Dependences. All of the calculations reported up to this point have been carried out with particle masses that yield a mass ratio (the incident particle mass to the liquid particle mass) of 0.348. Simple kinematic considerations, however, predict that the magnitude of the energy transfer will depend on this ratio.[37] In particular, the so-called "Baule formula", which has proved useful in characterizing the factors contributing to gas−solid energy transfer and has been used by Nathanson and co-workers[28,29] in interpreting their experimental energy distributions, predicts that the average energy transfer, ΔE, occurring when a particle having energy E_i collides with a surface at temperature T_l will be

$$\frac{\Delta E}{E_i} = \frac{4\mu}{(1+\mu)^2}(1/2)[1 - \cos\chi(1 - \mu^2 \sin^2\chi)^{1/2} + \mu \sin^2\chi][1 + (V - 2RT_l)/E_i]$$

Here the mass ratio is μ, the deflection angle $(180° - \theta_i - \theta_f)$ is χ, V is the depth of the gas−liquid potential well, the gas−liquid interaction is modeled as a simple square well, and R is the gas constant; the angle term corrects the two-body collision result for a distribution of impact parameters; the final energy term compensates for the acceleration of the incident particle when it is attracted by its collision partner, the latter vibrating harmonically with an energy characteristic of the surface temperature. It is important to keep in mind that this equation is derived assuming two-body, impulsive collisions with the last atom in a linear chain; thus, it provides only a general framework within which to discuss our simulation results. Nevertheless, it predicts that when χ vanishes (the probability of which is enhanced for normal incidence), the average energy transfer will be 72% for a system characterized by the parameters for which the energy distributions of Figure 4 were obtained. Our average energy transfer determined for that same system is 76%, so in this particular case the Baule formula even yields reasonably quantitative results.

Our principal interest here, though, is in the form of first quotient appearing in this equation. (The angle factor, although it does involve masses, is problematic in the present case given the broad scattering angle distributions presented above.) For small μ, this first factor yields a linear dependence of the energy transfer on the mass ratio. However, as that ratio approaches unity, the factor itself approaches unity, its maximum value, and one expects particularly efficient energy transfer to be observed. Even larger ratios would be expected to yield a decrease in the energy exchange if the equation remains valid, but in fact the dynamical assumptions inherent in this simple model are not strictly applicable under these circumstances. (The reader is referred to the discussion of the assumptions and limitations of the Baule formula given by Harris[37] for further elaboration of the model.)

We have investigated the energy transfer in our system for a series of projectile masses, isolating the effect of a change in the mass ratio by using the identical potential parameters in each case. (If the liquid is taken to be In, as discussed previously, then the projectile atoms correspond to Ne, Ar, Kr, In, and Pb. An additional mass combination was also included in order to extend the range of ratios considered; the mass of the projectile in this case was taken to be half of that of Ne.)

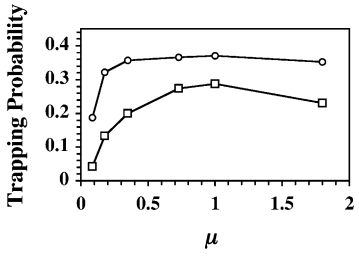

Figure 7. Calculated incident atom trapping probabilities as a function of the incident/surface atom mass ratio at $T^* = 0.72$ (squares) and 0.92 (circles). Error bars here are on the order of the size of the plot symbols.

The results of those simulations, focusing on the trapping probabilities, which are a measure of the net energy transfer, are shown in Figure 7. We see in these results just the general mass dependence expected if the collision dynamics indeed is strongly influenced by simple kinematics. At both liquid temperatures studied, the trapping probability increases rapidly at small values of μ, reaching a maximum at or near unit mass ratio, and decreasing slowly thereafter. Obviously, the Baule formula does not predict the difference between the results at the two temperatures; for the high incident atom energy used in this work, the energy factor that accounts for nonzero surface temperature and interaction energy does not vary enough (from 0.95 to 0.92) over this temperature range to explain the significant difference in the trapping probabilities, especially for small mass ratios. Moreover, the kinematic energy factor predicts that energy transfer should *decrease*, due to an increased probability that the surface species will impart its thermal energy to the impinging particle, as the liquid temperature increases. This discrepancy between the predictions of the simple kinematic model and the values obtained from our simulations is a natural consequence, though, of the temperature-dependent dynamical differences arising principally from variations in the surface roughness. Even so, we cannot ignore that with an increase in the liquid temperature also comes an increase in the equilibrium vapor pressure and an increase in the probability that the incident gas atom will collide with a vapor-phase species either before or after interacting with the liquid surface.

The remaining variable in the kinematic energy factor, the strength of the gas−liquid interaction potential, also deserves attention. Using the Lennard−Jones parameter, ϵ_{gl}, to approximate the square-well depth, V, one is led to expect that this interaction strength will have little effect on the average energy transfer when the initial kinetic energy of the incident atom is relatively large, as it is in the present study: increasing ϵ_{gl}^* (the Lennard−Jones gas−liquid well depth in the reduced units noted previously) from a value of 0.444, appropriate for the Ar−In system, to a value of 1.39 only produces a 5% change in the energy factor when the (reduced) liquid temperature is 0.72. To investigate the usefulness of this prediction in characterizing the dynamics of our system, we performed simulations using these two interaction strengths as well as two intermediate values. The results of these calculations are displayed in Figure 8.

We see in the upper panel that the general form of the scattered atom energy distribution is fairly insensitive to the change in the gas−liquid interaction considered here; in fact, the average final energy of the scattered atoms differs only by

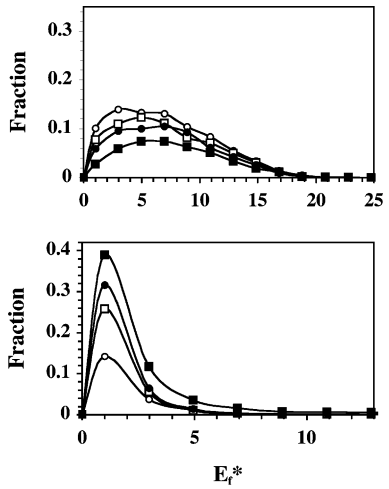

Figure 8. Final energy distributions of scattered (upper panel) and trapped (lower panel) particles determined for gas−liquid potential well depths (in reduced units) of 0.444 (open circles), 0.722 (open squares), 1.00 (solid circles), and 1.39 (solid squares). The mass ratio, μ, and reduced temperature, T^*, used in these simulations are 0.348 and 0.72, respectively.

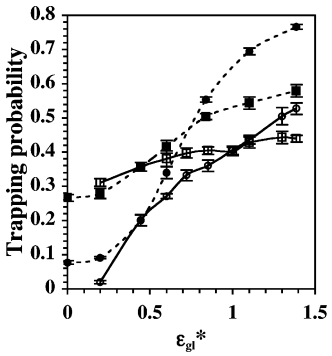

Figure 9. Dependence of the atom trapping probability on the gas−liquid interaction well depth in the simulations for which energy distributions are depicted in Figure 8 (open circles; $T^* = 0.72$) and also at a higher temperature (open squares; $T^* = 0.92$). The points in these data sets are shown connected by solid lines. The analogous results obtained by scaling only the attractive part of the Lennard−Jones potential energy function are shown with solid points, connected by dashed lines. Error bars correspond to one standard deviation.

about 11% over this range. More dramatic, though, is the overall effect, the average final kinetic energy of all incident species decreases by 31%, and especially the impact on the trapped-particle energy distribution. All of these distributions peak in the lowest energy "bin", of course, but the number of species that are essentially thermalized clearly increases. (All of the fractional occupations again refer to fractions of the 4000 total trajectories.) At this temperature and at $T^* = 0.92$, the trapping probabilities, which are shown in Figure 9, also attest to an increase in the efficiency of energy transfer. Although even the largest of these interaction energies is less than 8% of the incident atom's initial kinetic energy, the net energy transfer in this system is sufficiently great in general that the increased interaction energy is associated with a roughly linear increase in the probability that a temporarily trapped atom will be unable to escape the surface of the liquid. (For the trapping probabilities determined at $T^* = 0.72$, a linear fit to the results for $\epsilon_{gl}^* > 0.4$ yields $p_{trap} = 0.34\epsilon_{gl}^* + 0.07$, with R^2 equal to 0.99; at $T^* = 0.92$, a linear fit is less satisfactory, $p_{trap} = 0.086\epsilon_{gl}^* + 0.33$, with R^2 only equal to 0.94 in this case). Note that these linear (or nearly so) dependences on the well depth are precisely in the direction predicted by kinematics, although the magnitude of the effect is greatly enhanced in our prototypical system. (Departure of the trends at small ϵ_{gl}^* from the linearity predicted by the kinematic model is not particularly surprising given the dynamical differences between the $\epsilon_{gl}^* \rightarrow 0$ and $V \rightarrow 0$ limits, differences that are discussed below.)

At the higher temperature, however, the effect of increasing the interaction well depth is muted. Such a result would be predicted given the form of the Baule formula's energy factor: because the thermal energy of the surface atom is subtracted from the interaction well depth, increasing both tends to minimize the change in the calculated energy transfer. (Physically, the effect of an increase in the acceleration of the incident particle as it approaches the surface is offset by an increase in energy imparted to the impinging particle by the thermal motion of the surface atom.) An additional consideration enters here, however. If, as the surface becomes rougher due to an increase in the temperature of the liquid, the probability that an incoming particle will experience multiple scattering events increases, then relatively small changes (relative to the incident energy) in the interaction well depth will not alter the trapping probability appreciably.

Alteration of the Lennard−Jones parameter ϵ_{gl}^*, it must be remembered, yields both a change in the gas−liquid potential well depth and a change in the steepness of the short-range repulsive interaction. However, the kinematic model presumes that the repulsive interaction is just a hard wall, independent of the depth of the (square) potential well. We thus performed additional simulations in which we varied only the factor of ϵ_{gl}^* appearing in the r^{-6} term while keeping the r^{-12} term constant at the value used previously when $\epsilon_{gl}^* = 1$. The results of this work also are shown in Figure 9. Although the relative positions of the curves for the two temperatures are similar to what we found when varying ϵ_{gl}^* in both the attractive and repulsive parts of the gas−liquid potential function, the curves themselves are now distinctly sigmoidal in shape, with a nonzero trapping probability in the limit of zero well depth. Of course, the comparison with the kinematic model is not perfect here either: increasing the magnitude of the attractive term in the potential function also increases the width of the potential well and thus increases the number of surface species with which the incident atom is interacting simultaneously. Notable here is the fact that independently altering the strength of the attractive potential component yields higher trapping probabilities when $\epsilon_{gl}^* > 1$. Here the repulsive component of the potential is "softer" than it would be if the attractive and repulsive contributions were scaled uniformly, and the energy transfer is enhanced as a result.

IV. Concluding Remarks

Although a Lennard−Jones system affords an imperfect model of one of the gas−liquid scattering systems investigated to date or of a practical propellent, it nonetheless provides a dynamical benchmark against which more complex systems may be compared. One might expect that energy transfer in such a system would be prosaic, that the gap between the incident particle energy and the average thermal energy of the surface atoms is sufficiently great that thermalization of the incident species would be quite unlikely. Instead, even for the high incident atom kinetic energy considered here, we find that on the average the impinging species lose the majority of that energy upon collision with the surface, and that as a result a significant fraction of the species becomes trapped at the surface. It is notable that efficient energy transfer such as this also has been observed experimentally in HCl scattering from glycerol

by Nathanson and co-workers,[42] an observation that lends support to the notion that a simple Lennard−Jones system can capture the fundamental features of gas−liquid interfacial energy exchange.

Two particular results stemming from this work deserve highlighting. The first of these is that our calculations in general agree well with the predictions of a simple kinematic model of the dynamics, even when the conditions are such that the kinematic model might not strictly be applicable. Inasmuch as the model also has been shown to reproduce the behavior observed in gas−liquid scattering measurements, we believe that kinematics must dominate the dynamics in many of these systems. The kinematic model originally was devised to explain energy transfer in gas−solid collisions, and indeed it does so reasonably well in numerous systems.[36] Thus, it is tempting to conclude that much of the understanding of gas−solid energy transfer that emerged in the second half of the twentieth century will be applicable as well to processes occurring at a gas−liquid interface. If this transference is valid, then one obviates the need to treat gas−liquid energy exchange as a unique phenomenon and instead can concentrate on those particular features of liquid surfaces that really are distinctive.

One of these special features of liquid surfaces is the degree to which they are thermally roughened. This characterization constitutes the second of the key findings of the present work. The kinematic model of energy transfer in this system cannot adequately explain the notable dependence of the energy transfer and the incident-species' trapping probability on the temperature of the liquid. Doing so requires a change in the topology of the surface, that the surface becomes progressively rougher as the temperature of the bulk liquid is increased. As in the case of recognizing the overall dominance of kinematics in these systems, we are not the first to offer such an explanation: Nathanson and co-workers, in explaining the increased energy transfer with increasing liquid temperature in their experiments, also attributed the effect to surface roughening.[17,21,23] Here, though, we can correlate the effect with a change in the effective width of the surface layer and can confirm that roughening is accompanied by enhanced thermalization and trapping of the impinging species.

The next step in the study of gas−liquid interfacial dynamics is to move beyond the simple liquid model adopted here and to include structured molecules with internal degrees of freedom (and, consequently, additional pathways for depositing energy into the condensed phase). We currently are investigating collisions at the surface of liquid nitromethane, for which a good (although nonreactive) potential energy function exists.[43] Our initial indications are that the presence of internal degrees of freedom greatly enhances the energy transfer, but it is also important to assess the role that rotational excitation of the liquid molecules plays in the process. We have also begun an examination of a simple system in which collisional energy transfer can result in dissociation of the liquid molecule, the first step toward modeling reactive processes at a liquid surface.

Acknowledgment. We thank G. M. Nathanson and D. L. Thompson for helpful discussions and suggestions concerning this work. This work was supported by a DOD MURI grant managed by the Army Research Office.

References and Notes

(1) Miller, M. S. *Mater. Res. Soc. Symp. Proc.* **1996**, *418*, 169.
(2) Miller, M. S.; Anderson, W. R. *Prog. Astronaut. Aeronaut.* **2000**, *185*, 501.
(3) Miller, M. S. *Burning-Rate Models and Their Successors: A Personal Perspective*; ARL-TR-2996; U.S. Army Research Laboratory; Aberdeen Proving Ground, MD, 2003.
(4) Barker, J. A.; Auerbach, D. J. *Surf. Sci. Rep.* **1985**, *4*, 1.
(5) Rettner, C. T.; Auerbach, D. J.; Tully, J. C.; Kleyn, A. W. *J. Phys. Chem.* **1996**, *100*, 13021.
(6) See, for example, Feldman, L. C.; Mayer, J. W. *Fundamentals of Surface and Thin Film Analysis*; North-Holland: New York, 1986.
(7) Hurlbut, F. C.; Beck, D. E. *U. C. Eng. Proj. Report HE-150-166*; University of California, 1959.
(8) Sinha, M. P.; Fenn, J. B. *C. R. Symp. Int. Jets Mol., 5th* **1975**, Paper No B6.
(9) Balooch, M.; Siekhaus, W. J.; Olander, D. R. *J. Phys. Chem.* **1984**, *88*, 3521.
(10) Balooch, M.; Siekhaus, W. J.; Olander, D. R. *J. Phys. Chem.* **1984**, *88*, 3529.
(11) Balooch, M.; Siekhaus, W. J.; Olander, D. R. *J. Phys. Chem.* **1986**, *90*, 1671.
(12) Olander, D. R.; Balooch, M.; Siekhaus, W. J. *J. Phys. Chem.* **1986**, *90*, 4397.
(13) Balooch, M.; Olander, D. R.; Siekhaus, W. J. *Oxid. Met.* **1987**, *28*, 195.
(14) Olander, D. R.; Balooch, M.; Siekhaus, W. J. *High-Temperature Science* **1987**, *24*, 21.
(15) Saecker, M. E.; Govoni, S. T.; Kowalski, D. V.; King, M. E.; Nathanson, G. M. *Science* **1991**, *252*, 1421.
(16) King, M. E.; Nathanson, G. M.; Hanning-Lee, M. A.; Minton, T. K. *Phys. Rev. Lett.* **1993**, *70*, 1026.
(17) King, M. E.; Saecker, M. E.; Nathanson, G. M. *J. Chem. Phys.* **1994**, *101*, 2539.
(18) Nathanson, G. M. *Proc. Robert A. Welch Found. Conf. Chem. Res.* **1994**, *38th*, 187.
(19) Lipkin, N.; Gerber, R. B.; Moiseyev, N.; Nathanson, G. M. *J. Chem. Phys.* **1994**, *100*, 8408.
(20) Benjamin, I.; Wilson, M. A.; Pohorille, A.; Nathanson, G. M. *Chem. Phys. Lett.* **1995**, *243*, 222.
(21) Ronk, W. R.; Kowalski, D. V.; Manning, M.; Nathanson, G. M. *J. Chem. Phys.* **1996**, *105*, 4397.
(22) Nathanson, G. M.; Davidovits, P.; Worsnop, D. R.; Kolb, C. E. *J. Phys. Chem.* **1996**, *100*, 13007.
(23) King, M. E.; Fiehrer, K. M.; Nathanson, G. M.; Minton, T. K. *J. Phys. Chem. A* **1997**, *101*, 6556.
(24) Tribe, L.; Manning, M.; Morgan, J. A.; Stephens, M. D.; Ronk, W. R.; Treptow, E.; Nathanson, G. M.; Skinner, J. L. *J. Phys. Chem. B* **1998**, *102*, 206.
(25) Morris, J. R.; Behr, P.; Antman, M. D.; Ringeisen, B. R.; Splan, J.; Nathanson, G. M. *J. Phys. Chem. A* **2000**, *104*, 6738.
(26) Morgan, J. A.; Nathanson, G. M. *J. Chem. Phys.* **2001**, *114*, 1958.
(27) Manning, M.; Morgan, J. A.; Castro, D. J.; Nathanson, G. M. *J. Chem. Phys.* **2003**, *119*, 12593.
(28) Chorny, I.; Benjamin, I.; Nathanson, G. M. *J. Phys. Chem. B* **2004**, *108*, 995.
(29) Nathanson, G. M. *Annu. Rev. Phys. Chem.* **2004**, *55*, 231.
(30) Chase, D.; Manning, M.; Morgan, J. A.; Nathanson, G. M.; Gerber, R. B. *J. Chem. Phys.* **2000**, *113*, 9279.
(31) Muis, A.; Manson, J. R. *J. Chem. Phys.* **1997**, *107*, 1655.
(32) Muis, A.; Manson, J. R. *J. Chem. Phys.* **1999**, *111*, 730.
(33) Wilson, M. A.; Pohorille, A. *J. Phys. Chem. B* **1997**, *101*, 3130.
(34) See, for example, Allen, M. P.; Tildesley, D. J. *Computer Simulation of Liquids*; Oxford University Press: Oxford, U.K., 1992.
(35) Smith, W.; Forester, T. R. *DL_POLY_2*, version 2.14; CCLRC, Daresbury Laboratory: Daresbury, Warrington, U.K., 2003.
(36) See, for example, Zangwill, A. *Physics at Surfaces*; Cambridge University Press: Cambridge, U.K., 1988.
(37) Harris, J. Mechanical Energy Transfer in Particle-Surface Collisions. In *Dynamics of Gas−Surface Interactions*; Rettner, C. T., Ashfold, M. N. R., Eds.; Royal Society of Chemistry: Cambridge, U.K., 1991.
(38) Characterization of surface roughening is itself a topic of considerable interest. For recent contributions to this field, see Phillips, L. F. *J. Phys. Chem. B* **2001**, *105*, 11283; Phillips, L. F. *Acc. Chem. Res.* **2004**, *37*, 982; Phillips, L. F. *J. Phys. Chem. B* **2004**, *108*, 1986; and references therein.
(39) Logan, R. M.; Stickney, R. E. *J. Chem. Phys.* **1966**, *44*, 195.
(40) Logan, R. M.; Keck, J. C.; Stickney, R. E. *Rarefied Gas Dyn.* **1967**, *1*, 49.
(41) Tully, J. C. *J. Chem. Phys.* **1990**, *92*, 680.
(42) Ringeisen, B. R.; Muenter, A. H.; Nathanson, G. M. *J. Phys. Chem. B* **2002**, *106*, 4988.
(43) Agrawal, P. M.; Rice, B. M.; Thompson, D. L. *J. Chem. Phys.* **2003**, *119*, 9617.